Title: Molecular dissection of cobra venom highlights heparinoids as an antidote for spitting cobra envenomation

Authors: Tian Y. Du[1], Steven R. Hall[2], Felicity Chung[1], Sergey Kurdyukov[1], Edouard Crittenden[2], Karishma Patel[3], Charlotte A. Dawson[2], Adam P. Westhorpe[2], Keirah E. Bartlett[2], Sean A. Rasmussen[4], Cesar L. Moreno[1], Christopher E. Denes[1], Laura-Oana Albulescu[2], Amy E. Marriott[2], Joel P. Mackay[3], Mark C. Wilkinson[2], José María Gutiérrez[5], Nicholas R. Casewell[2]*, G. Gregory Neely[1]*

Affiliations:

[1] Charles Perkins Centre, Dr. John and Anne Chong Lab for Functional Genomics, and School of Life and Environmental Sciences, University of Sydney, Camperdown, New South Wales, Australia 2250.

[2] Centre for Snakebite Research and Interventions, Department of Tropical Disease Biology, Liverpool School of Tropical Medicine, Pembroke Place, L3 5QA Liverpool, UK.

[3] School of Life and Environmental Sciences, The University of Sydney, Sydney, Australia 2008.

[4] Department of Pathology and Laboratory Medicine, Queen Elizabeth II Health Sciences Centre and Dalhousie University, 7th Floor of MacKenzie Building, 5788 University Avenue, Halifax, Nova Scotia, B3H 1V8, Canada.

[5] Clodomiro Picado Institute, School of Microbiology, University of Costa Rica, P.O. Box 15501, San José, Costa Rica 11501-2060.

*Corresponding author. Email: greg.neely@sydney.edu.au or nicholas.casewell@lstmed.ac.uk

OVERLINE: SNAKEBITE

One-Sentence Summary: Spitting cobra venom cytotoxins use a common heparin-sensitive mechanism to cause tissue damage**.**

Editor's summary:

Abstract: Snakebite affects about 1.8 million people annually. The current standard of care involves antibody-based antivenoms, which can be difficult to access and are generally not effective against local tissue injury, the primary cause of morbidity. Here we used a pooled whole genome CRISPR knockout screen to define human genes that, when targeted, modify cell responses to spitting cobra venoms. A large portion of modifying genes that confer resistance to venom cytotoxicity were found to control proteoglycan biosynthesis, including *EXT1*, *B4GALT7*, *EXT2*, *EXTL3*, *XYLT2*, *NDST1* and *SLC35B2* which we validated independently. This finding suggested heparinoids as possible inhibitors. To this end, we show that heparinoids prevent venom cytotoxicity and mechanistically this occurs though binding three-finger cytotoxins. Critically, the FDA-approved heparinoids tinzaparin was found to reduce tissue damage in vivo when given via a medically relevant route and dose. Overall, our systematic molecular dissection of cobra venom mechanisms provides insight into how we can treat cobra envenomation, information that can help improve the lives of millions of people worldwide.

Introduction

Snakebites kill an estimated ~138,000 people each year, with another ~400,000 people experiencing devastating long-term morbidity (*1*). Most of these envenomings occur in Sub-Saharan Africa and South or Southeast Asia and disproportionately impact young adults and children (*2*, *3*). This makes snakebite envenoming the deadliest of the neglected tropical diseases (NTDs) with its burden landing mainly on impoverished rural communities (*4*). The resulting annual disease burden from snakebite in West Africa and Southeast Asia alone amounts to about 319,000 and about 392,000 disability adjusted life years (DALYs), respectively, with associated costs for the latter (2.5 billion USD) representing 0.1% of the region's GDP (*5*). Consequently, the World Health Organization (WHO) recently elevated snakebite to a 'priority category A NTD' and announced the goal of reducing the global burden of snakebite in half by 2030 (*6*).

Most current available treatment for snakebite envenoming are antibody-based antivenoms derived from the immunisation of donor animals such as horse and sheep (*7*,*8*). Although lifesaving, this centuries old technology is species specific, requires cold storage, and must be administered intravenously in hospital settings. Moreover, antivenoms can induce adverse reactions and are often prohibitively expensive even if available (*9*,*10*). Importantly, antivenoms are also ineffective against severe local envenoming due to the large size of antibodies and their fragments meaning these treatments are unable to effectively block local tissue injury (*11*,*12*). Local envenomation events cause painful progressive swelling, blistering or tissue necrosis and can lead to loss of limb function, amputation, and lifelong disability (*12*). Unfortunately, there has been considerably less research on these tissue damaging effects than on the neurotoxic and haemotoxic effects of venoms despite being the leading cause of morbidity. Of the two major medically important venomous snake families, elapids and viperids, based on these severe morbidity-causing pathologies, the WHO lists many cobras (*Naja* spp.) as "Category 1" species of highest medical importance *(6, 11-12)*.

Progress has been made to elucidate the mechanisms underlying local tissue damage (see review, *13*), with a focus on repurposing drugs that can more quickly be administered on the field (*14*). However, a basic molecular understanding of how diverse snake venoms interact with human physiology is required to inform the development of these new therapeutics (*15*). Here we used a functional genomics approach to define venom-target genetic interactions that modify cytotoxicity and then used this information to develop a locally acting venom antidote.

Results

Whole genome CRISPR knockout screens for spitting cobra venom cytotoxicity

We first tested the cytotoxicity of red (*N. pallida*, Tanzania) and black-necked (*N. nigricollis*, Nigeria) spitting cobra venom from Sub-Saharan Africa (see geographical distribution in **Fig. 1A**) on the human haploid cell line, HAP1 (**Fig. 1B**). Additional pharmacological inhibition of apoptosis through the caspase-3 inhibitor Ac-DEVD-Cho or pan caspase inhibitor Z-VAD-FMK did not suppress venom cytotoxicity, however the necroptotic inhibitor necrosulfonamide (NSA) limited some cell death, suggesting cobra venom cytotoxicity may partially trigger necroptotic death (**fig. S1A**). To guide the development of therapeutics, we sought to define the molecular

mechanisms involved in venom-induced cell death using whole genome CRISPR knockout (KO) screening (**Fig. 1C**). HAPI cells were transduced with the TKOv3 library, which targets most human protein-coding genes, with about 4 guides/gene (*16*). This pool of CRISPR KO cells was then selected with 5 µg/mL of *N. pallida* or *N. nigricollis* venom for a total of nine days. Single guide RNA in surviving cells was isolated, amplified by PCR, and quantified by next generation sequencing. Guide enrichment was compared to a control unselected population using the MaGeCK pipeline (*17*). Guide RNAs associated with venom sensitization (Log_2<-2, FDR<0.1) or resistance (Log_2>2, FDR<0.1) were identified, and substantial overlap was observed between the two snake species (**Fig. 1, D** and **E, fig. S2, A** to **D, data files S1** and **S2**).

For *N. pallida* venom, the top significant genes that, when targeted, promoted venom sensitization include the chromatin remodelling SWI/SNF component *SMARCD1* (*18*), the cyclin dependent kinase *CDK13* (*19*), the histone deacetylase *HDAC3* (*20*), the anti-apoptotic protein *ZFAT* (*21*), and *CRAMP1L*, an uncharacterised gene linked with susceptibility to skin rash (*22*) (**data file S1**). For *N. nigricollis* venom, the top sensitizers included the cell growth/tumour suppressors *TSC1* and *TSC2* (*23*), the TSC subunit *TBC1D7* (*24*), the SWI/SNF component *SMARCC1* (*25*), the lipid phosphatase Inositol Polyphosphate Phosphatase Like 1 (*INPPL1*), which encodes the protein SHIP2 (*26*), and the microtubule interaction protein *APPBP2* (*27*) (**data file S2**).

For *N. pallida* venom, the top significant genes that, when targeted, promoted venom resistance included the uncharacterized transmembrane protein *TMEM50A*, the suppressor of growth hormone tetraspanin membrane protein *LEPROTL1* (*28*), and components of proteoglycan biosynthesis *NDST1*, *XYLT2*, *EXT1*, *EXTL3*, and *SLC35B2* (*29*) (**data file S1**). For *N. nigricollis* venom, the top promoters again included *LEPROTL1* and *TMEM50A*, as well as multiple components of the proteoglycan biosynthesis machinery including *EXT1, B4GALT7, EXT2, EXTL3, XYLT2, NDST1* and *SLC35B2* (**data file S2**). Further, pathway analysis of these data highlighted heparin sulfate, chondroitin sulfate, and dermatan sulfate biosynthesis as critical pathways required for cytotoxicity of both *N. pallida* and *N. nigricollis* venoms (**Fig. 1, F** and **G**). The top pathway for both venoms was heparan/heparin sulfate biosynthesis (*N. pallida*: $p<10^{-10}$, *N. nigricollis*: $p<10^{-8}$) and our screening data showed that targeting of most of the heparan/heparin sulfate biosynthesis pathway components individually was sufficient to block venom activity (*N. pallida* 7/11, and *N. nigricollis* 8/11 components of the pathway were hit, see **fig. S2E**).

Heparin biosynthesis is required for venom cytotoxicity

To validate these results, we generated single KO cell pools with sgRNAs that targeted each resistance gene individually (**data file S3**) and tested cytotoxicity. Targeting each component of the heparan/heparin biosynthesis pathway conferred some resistance to each venom (**Fig. 2, A and B**), confirming a role for heparan in cobra venom cytotoxicity. To test the generalizability of this requirement, we also treated gene-targeted cells with venom from an additional spitting cobra species (**Fig. 2C, fig. S3A**; Tanzanian *N. nigricollis*), and again showed that components of heparan/heparin sulfate biosynthesis were required for cytotoxicity.

Heparan and heparin sulfate share a sugar backbone synthesized by a common pathway (**fig. S2E**). Whereas heparan sulfate is a ubiquitous component of the extracellular matrix, heparin is primarily produced by tissue mast cells. Heparin is a highly sulfated, polyanionic polysaccharide used clinically for its potent anticoagulant activity. Heparin is on the WHO Model List of Essential Medicines (EML), however, multiple low molecular weight (LMW) medical variants of heparin

(tinzaparin, T; dalteparin, D) termed “heparinoids" are also available and approved for antithrombotic use (*30, 31*) (**Fig. 3A**). Since heparan/heparin sulfate biosynthesis was necessary for venom to cause cytotoxicity, we hypothesized that adding excess free heparin or LMW heparinoids may be sufficient to block venom cytotoxicity. Indeed, immediate treatment with heparin, tinzaparin, or dalteparin, all blocked cytotoxicity in response to *N. pallida* (**Fig. 3B**, quantified in **3C**), Nigerian *N. nigricollis* (**Fig. 3B**, quantified in **3D**), or Tanzanian *N. nigricollis* (**Fig. 3E**) venom, and the related non-anticoagulant heparinoid N-acetyl-heparin *(32)* showed similar effects (**Fig. 3F**).

To test if heparinoids could block venom cytotoxicity therapeutically, we first treated cells with *N. nigricollis* venom and then added heparin over time. Addition of heparin or tinzaparin up to 60 minutes after venom could still block Nigerian *N. nigricollis* venom cytotoxicity (**Fig. 3G, fig. S3B**), although protection was lost at 90 minutes. Heparin or tinzaparin treatment after *N. pallida* and Tanzanian *N. nigricollis* venom could also block cytotoxicity (**fig. S3, C to F).**

Heparinoids prevent venom interaction with the cell surface

Because heparan sulfate and related molecules bind soluble effectors including growth factors and proteases *(33, 34),* we hypothesized that in the context of its venom antidote activity, heparin may act as a “decoy” venom receptor and block venom-cell interactions. To test this hypothesis, we labelled each cobra venom with an Alexa-488 fluorophore and then evaluated venom-cell interactions by flow cytometry. Whereas labelled cobra venom showed a strong interaction with untreated cells (*N. pallida* venom shown in **Fig. 4A**), adding heparin (**Fig. 4B**) or tinzaparin (**Fig. 4C**) blocked venom-host cell interactions. These data are quantified in **Fig. 4D**, and similar results were observed for venom from the two geographical variants of *N. nigricollis* (**fig. S4, A to H**). Thus, free heparin could suppress venom-target interactions, and this was sufficient to block cytotoxicity.

Heparin interacts with three-finger cytotoxins to block venom-host interactions

Snake venoms are variable mixtures of different toxins, and cobra venoms consist predominantly of multiple isoforms of phospholipases A2 (PLA_2) and three-finger toxins (3FTx) (*35*). To identify which specific venom components interact with heparinoids, we separated *N. pallida* (**Fig. 4, E** and **F**) and *N. nigricollis* (**fig. S5, A** and **B**) venom using heparin affinity chromatography. Most of the venom material bound to the column and was eluted in 3-4 main peaks (**Fig. 4E, fig. S5, A** and **B**), suggesting that heparin may interact with multiple venom components. The main proteins comprising each peak were identified by liquid chromatography mass spectrometry (LC-MS): P1 (weak heparin interaction) contained mainly acidic PLA_2, P2 (moderate heparin interaction) contained the 3FTx cytotoxin 1 (CTx1), and P3 (strong heparin interaction) contained both basic PLA_2 ($bPLA_2$) and the 3FTx cytotoxins CTx3 and 4 (**data files S4 to S10**). We then further fractionated P3 using cation exchange to separate basic PLA_2 ($bPLA_2$) from the 3FTx cytotoxins CTx3 and 4 (**Fig. 4F** and **fig. S5C)** and assessed the purity of each fraction on SDS-PAGE (**Fig. 4G**, **fig. S5, D** and **E**).

Isolated *N. pallida* toxins were then subjected to surface plasmon resonance (SPR) to assess binding affinity with heparin, dalteparin and tinzaparin. Heparin bound with high affinity to CTx3 (K_D = 37 nM) and CTx4 (K_D = 36 nM), bound weakly to $bPLA_2$ (K_D >100 nM) and exhibited no specific binding to CTx1 or PLA_2 (**Fig. 4, H and I**). The same pattern of binding is observed for

tinzaparin and dalteparin (**fig. S6**). Functionally, the 3FTxs CTx3 and 4 were highly cytotoxic and, in line with their binding profile, their activity was inhibited by heparin (**Fig. 4J**). Although CTx1 also showed strong cytotoxicity, this activity was not heparin sensitive (**Fig. 4J**). Similar binding, cytotoxicity and inhibition data were obtained for the two *N. nigricollis* venoms (**fig. S7** and **fig. S8**), with CTx3 and 4 demonstrating the most potent heparinoid binding properties. Collectively, these data demonstrated that heparin and related compounds could block African spitting cobra venom cytotoxicity by acting directly on the cytotoxic 3FTxs CTx3 and 4.

To assess the breadth of this anti-venom activity, we tested the ability of heparin to block other cytotoxic snake venoms (**Fig. 4, K to O**). We found both heparin and N-acetyl-heparin (**fig. S9**) could suppress cytotoxicity caused by venom from the monocled cobra (**Fig. 4K**; *Naja kaouthia*), the Chinese cobra (**Fig. 4L**; *Naja atra*), and the Indian spectacled cobra (**Fig. 4M**; *Naja naja*). However, neither had the ability to block cytotoxicity caused by West African saw-scaled viper (**Fig. 4N**; *Echis ocellatus*) or African puff adder (**Fig. 4O**; *Bitis arietans*) venom (see also **fig. S9**). This is consistent with the fact that cobra venoms contain cytotoxic 3FTxs (*35*), whereas viper venoms do not (*36*). Overall, these data showed that heparin and LMW heparinoid drugs could inhibit cytotoxic 3FTxs and suggested that they may function as a potential antidote for cobra venoms.

Heparinoids protect against spitting cobra venom-induced skin damage

We next investigated whether heparin or heparinoids could protect human epidermal keratinocytes from *N. pallida* and *N. nigricollis* (Nigerian and Tanzanian) venom-induced cytotoxicity. Venom from each snake species induced cell death in a concentration-dependent manner (**Fig. 5A**), and treatment with heparinoids promoted cell survival (**Fig. 5B**) and inhibited cell death (**Fig. 5C**). We next tested the ability of heparinoids to block venom-induced dermonecrosis in vivo using a WHO-recommended preclinical model of local envenoming (*37–39*). Mice were intradermally (ID) dosed with venom from *N. pallida*, Nigerian *N. nigricollis*, or Tanzanian *N. nigricollis* (25, 57, and 63 µg, respectively), preincubated with saline vehicle or the heparinoids dalteparin or tinzaparin (60 µg [3 mg/mL]) (**Fig. 5D**). Although animals injected with venom-plus-vehicle exhibited large dermonecrotic lesions, animals that received venom-plus-dalteparin or -tinzaparin showed significant ($P<0.05$) reductions in lesion sizes, irrespective of the venom or drug tested (**Fig. 5E** and **fig. S10**, quantified in **Fig. 5, F to H**). Tinzaparin provided the greatest reduction in dermonecrosis across the three venoms (mean lesion size reduction of 94% versus 63% with deltaparin). For these reasons, we progressed tinzaparin into further rescue studies that better reflect envenoming by delivering treatment after venom dosing (**Fig. 5I**).

We used Tanzanian *N. nigricollis* venom for rescue studies because it was the most dermonecrotic of the three venoms tested (**Fig. 5H**) and we evaluated the efficacy of ID tinzaparin delivered immediately after venom injection. Both a low dose (3 mg/kg) and moderate 'human-equivalent' dose (21.5 mg/kg) of tinzaparin significantly ($P<0.05$) reduced the resulting mean sizes of venom-induced dermonecrotic lesions by 66 and 60%, respectively (**Fig. 5J, fig. S11**, quantified in **Fig. 5K**). Because tinzaparin is FDA-approved for subcutaneous (SC) daily dosing, we next challenged mice with the same ID venom dose before immediately delivering tinzaparin SC to a site underneath where venom was injected. Although the low (3 mg/kg) tinzaparin dose did not significantly reduce the mean size of dermonecrotic lesions, the moderate (21.5 mg/kg) dose of SC tinzaparin significantly ($P<0.01$) reduced the size of venom-induced dermonecrotic lesions by 50% (**Fig. 5L, fig. S11**, quantified in **Fig. 5M**) Histopathological analysis of skin tissue samples

collected from mice injected with Tanzanian *N. nigricollis* venom revealed prominent damage to all skin layers, with ulceration of the epidermis and necrosis of the underlying dermis, hypodermis and panniculus carnosus, whereas mice injected with venom and tinzaparin, either preincubated or delivered SC, showed reduction in epidermal ulceration and underlying necrosis (**Fig. 5N**). Overall, these data showed that heparinoid drugs can act to prevent severe local spitting cobra envenoming by blocking the cytotoxic actions of the 3FTx cytotoxins CTx3 and 4.

DISCUSSION

Defining the essential molecular interactions between cytotoxic venoms and target cells provides fundamental understanding of how these venoms act and how we can treat them medically. Here we described multiple critical genes and pathways required for cobra venom cytotoxicity, and for one pathway, heparan/heparin biosynthesis, we characterized this interaction in detail. Our unbiased approach led to the discovery of heparinoids as a pre-clinically effective cobra envenoming antidote. Further, we showed that heparinoids act by binding to and blocking 3FTx cytotoxicity, and cytotoxic 3FTx inhibitors represent a much-needed class of therapeutic (*14*). Overall, the results of this study provide insight into the mechanisms underlying cobra venom cytotoxicity, information that may be used to help reduce morbidity caused by snakebite envenomings.

Although antibody-based antivenoms are lifesaving therapies, there are issues with safety, specificity, and administration that impact their effectiveness. While progress has been made to generate broader acting recombinant antivenoms (*40*), systemic administration of antibody-based therapies are ineffective at preventing severe local envenoming (*1, 8, 12*). This is likely because of the rapid onset of snake venom-mediated cytotoxicity, delays in reaching a clinical environment, and the difficulty for centrally delivered antibodies to rapidly penetrate peripherally injured tissue. 3FTxs are highly abundant components of elapid venoms characterised by three loops that connect to a central core. These low molecular mass proteins (~6-9 kDa) have diverse neurotoxic, cardiotoxic and cytotoxic effects (*41*). In the context of spitting cobras, 3FTxs are highly cytotoxic and cause local tissue necrosis in snakebite victims (*42*). Thus, there is a strong need for the development of cheap, stable anti-3FTx therapeutics that can be rapidly administered on-site soon after a snakebite (*8*).

This study demonstrates that heparinoids may have utility in treating cobra bites from diverse regions of Africa and Asia. Although some snakebites cause venom-induced consumption coagulopathy (VICC), and use of heparin may be dangerous in these cases, spitting cobras are rarely, if ever, responsible for VICC *(43)*. Further, several clinical trials have been conducted where snakebite patients presenting with a coagulopathy received anticoagulant heparinoids, and no concerning safety signals relating to worsening coagulopathy or increased bleeding events were observed in these trials *(44–47)*. Moreover, both anticoagulant and non-anticoagulant heparinoids blocked cobra venom cytotoxicity suggesting that the antivenom activity of heparinoids is independent of anticoagulation. Tinzaparin showed particularly strong translational promise because it is an FDA-approved therapeutic (*30*). The potential for rapid community-level heparinoid administration therefore may hold promise for preventing morbidity caused by cobra bites.

Overall, our findings that tinzaparin could prevent dermonecrosis in a post-envenoming context align with studies investigating the Chinese cobra (*N. atra*) 3FTx cardiotoxin (*48*, *49*), as well as several studies using compositionally distinct viper venoms that suggest a protective effect by heparin. For example, preincubation with heparin reduced local skin lesions caused by Russell's viper (*Daboia russelii*) venom (*50*), and also blocked jararacussu (*Bothrops jararacussu*) PLA_2 myotoxin II damage to muscle or endothelial cells (*51-54*). Our work reaffirms the protective action of heparin and related compounds, extending it to cytotoxic 3FTxs and providing a molecular mechanism for this activity. Beyond venoms, cellular heparan sulfate has also recently been shown to be essential for SARS-CoV-2 infection (*55*). Here as well, use of free heparin or related compounds was sufficient to block infection, and similar observations have been made with other viral and bacterial pathogens (*56–59*). Heparan sulfate proteoglycans are conserved and widely expressed on the cell surface (*60*). Thus, targeting these molecules may be an optimal evolutionary strategy to interact with a broad range of species. Conversely, by providing this structure in excess, free heparin/heparinoids may act as a decoy target for multiple unrelated environmental hazards. Overall, the emerging molecular evidence suggests that heparan sulfate is a common cellular entry point for diverse human threats, and that heparinoids may have broad activity to protect us.

Our study does have limitations. While effective, tinzaparin when given therapeutically could not completely block dermonecrosis. Therefore more preclinical development, including dosing, delivery route, and combinations with other toxin-targeting drugs *(37, 61)* may be required to generate a fully effective local antidote. Moreover, our screening was performed in a cell line derived from a chronic myelogenous leukemia cell line, and further insight into cobra venom cellular targets could be achieved by additional CRISPR screening using a human skin cell line. Although we focused on heparan/heparin biosynthesis, our screening identified multiple other genes that may modify venom cytotoxicity that have yet to be investigated. Lastly, cytotoxicity is only one physiologically relevant impact of snake envenoming, and further CRISPR screening using other functional readouts beyond cell death may provide a more comprehensive understanding of mechanisms of action underlying envenomation.

To date, much of modern molecular medicine has focused on health challenges facing high income countries; however, here we applied these same approaches to understand snakebite envenoming, a substantial neglected tropical disease. From these efforts, we identified multiple new genes and pathways essential for snake venom cytotoxicity including heparan/heparin sulfate biosynthesis. Using this knowledge, we discovered that heparinoids can prevent cobra venom-associated dermonecrosis, suggesting this class as a potential therapy for spitting cobra envenomation.

Materials and Methods

Study design

The objective of this study was to identify the human genes and pathways that *Naja pallida* and *Naja nigricollis* venoms interact with to inform the development of therapeutics for spitting cobra envenomation. This was achieved through an unbiased whole genome CRISPR KO screen, with the lead pathway of heparan sulfate further validated genetically through single KO pools and pharmacologically through heparinoids. Heparinoid affinity to 3FTx was then determined. For in vivo studies, the WHO-recommended preclinical model for local envenoming was followed. Groups of 5 mice were randomly allocated into each treatment group based on sample sizes previously used to assess venom inhibition in this model. Experimenters were not blinded to the venom or treatment doses. A single lesion measurement from the venom-plus-PBS control group was excluded.

Venoms

Venoms were sourced from wild caught or captive bred snakes maintained in the herpetarium of the Liverpool School of Tropical Medicine's (LSTM) Centre for Snakebite Research Interventions (CSRI; United Kingdom). This facility and its protocols for the husbandry of snakes are approved and inspected by the UK Home Office and the LSTM and University of Liverpool Animal Welfare and Ethical Review Boards. The venom pools were from: East African *Naja nigricollis* (Tanzanian, TZN), West African *Naja nigricollis* (Nigerian, NGA), *Naja pallida* (Tanzanian), captive bred *Naja kaouthia*, *Naja atra*, and *Naja naja*, *Echis ocellatus* (Nigerian), and *Bitis arietans* (Nigerian). Crude venoms were lyophilized and stored at -20 °C. Prior to use, venoms were resuspended to 10 mg/ml in DPBS and stored at -80 °C in small aliquots with freeze-thaw cycles minimized to prevent degradation.

Animal ethics and maintenance

Liverpool, UK: All drug-plus-venom precincubation and ID-envenoming followed by SC-drug dosing animal experiments were conducted using protocols approved by the Animal Welfare and Ethical Review Boards of the Liverpool School of Tropical Medicine and the University of Liverpool and were performed in pathogen-free conditions under licensed approval (PPL #P58464F90) of the UK Home Office and in accordance with the Animal [Scientific Procedures] Act 1986 and institutional guidance on animal care. All experimental animals (18-28 g [4-6 weeks old], male, SWISS (CD-1) mice from Janvier, France or Charles River, UK) were acclimated for a minimum of one week before experimentation with their health monitored daily. Mice were grouped in cages of five, with room conditions of approximately 22 °C at 40-50% humidity, with 12/12 hour light cycles, and given ad lib access to CRM irradiated food (Special Diet Services, UK) and reverse osmosis water in an automatic water system. Mice were housed in specific-pathogen free facilities in Techniplast GM500 cages containing Lignocell bedding (JRS,

Germany), Sizzlenest zigzag fibers as nesting material (RAJA), and supplied with environmental enrichment materials.

San José, Costa Rica: All ID-envenoming followed by ID-drug dosing animal experiments were carried out at Instituto Clodomiro Picado. These were conducted using protocols approved by the Institutional Committee for the Care and Use of Laboratory Animals (CICUA) of the University of Costa Rica (approval number CICUA 82-08). All experimental animals (18-20 g [4-5 weeks old], mixed sex, CD-1 mice, Instituto Clodomiro Picado, Costa Rica) were acclimatized before experimentation. Mice were grouped in cages of five, with room conditions of approximately 22-24 °C at 60-65% humidity, with 12/12 hour light cycles, given ad lib access to food and water, and housed in Tecniplast Eurostandard Type II 1264C cages.

Preclinical anti-dermonecrosis efficacy of heparinoids via a preincubation model of envenoming

The in vivo experimental design was based on 3R-refined WHO-recommended envenoming protocols (*37–39*) and the anti-dermonecrosis methods were based on the Minimum Necrotizing Dose (MND) principles originally described in Theakston and Reid (*38*). As similar experiments with heparinoids as dermonecrosis treatments have never been performed previously, *a priori* power calculations were not possible; therefore, groups of 5 mice were randomly allocated into each treatment group based on sample sizes previously used to assess venom inhibition in this model (*37*, *62*). These groups of five mice (n=5; 45 mice total) received, in random order by a treatment-preparer separate from the treatment-injectors, experimental doses per mouse that consisted of venom from TZN *N. pallida* (25 µg), TZN *N. nigricollis* (63 µg), or NGA *N. nigricollis* (57 µg) combined with saline vehicle control, tinzaparin or dalteparin (60 µg [3 mg/kg]). Albulescu, *et al*. previously used 60 µg per 20 g mouse (3 mg/kg) of marimastat in their preclinical ID haemotoxicity trials (*39*); therefore this same comparative mg/kg concentration was chosen for our heparinoid dermonecrosis trials. In vivo team members were unblinded to the treatment randomisation post-injection to allow for the appropriate observation of venom-specific systemic endpoints that would have necessitated the implementation of early euthanasia. Stock solutions of tinzaparin and dalteparin were dissolved in PBS (50 mg/mL) and stored at -20 ºC prior to use in these in vivo experiments. All experimental doses were prepared to a volume of 50 µL and preincubated at 37 °C for 30 minutes the morning of the experiments, then kept on ice for no more than 3 hours until the mice were injected. For dose delivery, mice were briefly anesthetized using inhalational isoflurane (4% for induction of anesthesia, 1.5-2% for maintenance) and ID-injected in the shaved rear quadrant on the dorsal side of the flank skin with the 50 µL treatments. The mice were observed at least three times daily up to 72 hours post-injection to ensure signs of systemic envenoming or excessive external lesion development did not present. At the end of the experiments (72 hours) the mice were euthanized using rising concentrations of CO_2, after which the skin surrounding the injection site was dissected and the width and height of internal skin lesions measured with calipers, from which area was calculated, and photographed. Cross-section strips down the middle of the skin lesions were cut with microtome blades, placed in tissue cassettes, and preserved in 10% neutral formalin (BAF-6000-08A; CellPath) before being prepared for downstream histopathological analysis as previously described (*37*).

Preclinical anti-dermonecrosis efficacy of drug combinations via SC and ID 'rescue' models of envenoming

SC-drug rescue (UK): Groups of five mice (20 mice total) were ID-injected with TZA *N. nigricollis* venom (63 µg) diluted in 25 µL of PBS, followed by an immediate 25 µL SC-injection of either: (i) vehicle control (PBS), (ii) 3 mg/kg tinzaparin, or (iii) 21.5 mg/kg of tinzaparin (calculated human equivalent dose (*63*) based on therapeutic dose of tinzaparin in humans being 175 IU/kg (*64*) [roughly 1.75 mg/kg]), directly underneath the ID-injected venom. After 72 hours mice were euthanized by CO_2 inhalation, the skin surrounding the injection site was dissected, and the internal necrotic lesions were measured and photographed as described above. Separate (n=5) venom-plus-PBS control groups were completed for both the 3 and 21.5 mg/kg tinzaparin trials and data were combined due to being identical treatments.

ID-drug rescue (Costa Rica): Groups of five mice (20 mice total) were pre-treated with the analgesic tramadol (50 mg/kg by the subcutaneous route). Fifteen minutes later, mice were ID-injected with venom from TZA *N. nigricollis* (63 µg) diluted in 25 µL of PBS, after which they were immediately ID-injected in the same location with 25 µL of tinzaparin vehicle control (PBS) or 3 or 21.5 mg/kg of tinzaparin. After 72 hours mice were euthanized by CO_2 inhalation, the skin surrounding the injection site was dissected, and the internal necrotic lesions were measured and photographed as described above. Separate (n=5) venom-plus-PBS control groups were completed for both the 3 and 21.5 mg/kg tinzaparin trials and were combined due to being identical treatments. A single lesion measurement from the venom-plus-PBS control group was excluded as only a minor lesion developed in a mouse that we suspect of being misinjected, and thus did not receive the correct venom dose. This data point was formally identified as an outlier based on a Grubb's outlier test (Alpha = 0.2) (*65*), but to ensure transparency, images of this lesion are displayed in **fig. S11**.

Statistical analysis

Statistical analyses of data, unless otherwise stated, were conducted using GraphPad Prism (9.3.1) software. All error bars in this manuscript report SEM. A P value below 0.05 was considered significant. Specific statistical tests used for each dataset are stated in respective figure legends. All flow cytometry data was analyzed using FlowJo Software v10.6 (BD Life Sciences).

List of Supplementary Materials

Supplementary Materials and Methods

Figs. S1 to S11

References (*66* - *70*)

Data files S1 to S12

References and Notes

1. J. M. Gutiérrez, J. J. Calvete, A. G. Habib, R. A. Harrison, D. J. Williams, D. A. Warrell, Snakebite envenoming. *Nat Rev Dis Primers*. **3**, 17079 (2017).

2. J. Le Geyt, S. Pach, J. M. Gutiérrez, A. G. Habib, K. P. Maduwage, T. C. Hardcastle, R. Hernández Diaz, M. L. Avila-Aguero, K. T. Ya, D. Williams, J. Halbert, Paediatric snakebite envenoming: recognition and management of cases. *Arch. Dis. Child.* **106**, 14–19 (2021).

3. V. Y. Kshirsagar, M. Ahmed, S. M. Colaco, Clinical profile of snake bite in children in rural India. Iran. J. Pediatr. 23, 632–636 (2013).

4. R. A. Harrison, A. Hargreaves, S. C. Wagstaff, B. Faragher, D. G. Lalloo, Snake envenoming: a disease of poverty. PLoS Negl. Trop. Dis. 3, e569 (2009).

5. A. G. Habib, A. Kuznik, M. Hamza, M. I. Abdullahi, B. A. Chedi, J.-P. Chippaux, D. A. Warrell, Snakebite is Under Appreciated: Appraisal of Burden from West Africa. *PLoS Negl. Trop. Dis.* **9**, e0004088 (2015).

6. D. J. Williams, M. A. Faiz, B. Abela-Ridder, S. Ainsworth, T. C. Bulfone, A. D. Nickerson, A. G. Habib, T. Junghanss, H. W. Fan, M. Turner, R. A. Harrison, D. A. Warrell, Strategy for a globally coordinated response to a priority neglected tropical disease: Snakebite envenoming. *PLoS Negl. Trop. Dis.* **13**, e0007059 (2019).

7. R. A. Harrison, G. O. Oluoch, S. Ainsworth, J. Alsolaiss, F. Bolton, A.-S. Arias, J.-M. Gutiérrez, P. Rowley, S. Kalya, H. Ozwara, N. R. Casewell, Preclinical antivenom-efficacy testing reveals potentially disturbing deficiencies of snakebite treatment capability in East Africa. *PLoS Negl. Trop. Dis.* **11**, e0005969 (2017).

8. R. H. Clare, S. R. Hall, R. N. Patel, N. R. Casewell, Small Molecule Drug Discovery for Neglected Tropical Snakebite. *Trends Pharmacol. Sci.* **42**, 340–353 (2021).

9. N. Brown, J. Landon, Antivenom: the most cost-effective treatment in the world? Toxicon 55, 1405–1407 (2010).

10. H. A. de Silva, N. M. Ryan, H. J. de Silva, Adverse reactions to snake antivenom, and their prevention and treatment. Br. J. Clin. Pharmacol. 81, 446–452 (2016).

11. J. M. Gutiérrez, J. J. Calvete, A. G. Habib, R. A. Harrison, D. J. Williams, D. A. Warrell, Snakebite envenoming. *Nat Rev Dis Primers* **3**, 17063 (2017).

12. M. Rivel, D. Solano, M. Herrera, M. Vargas, M. Villalta, Á. Segura, A. S. Arias, G. León, J. M. Gutiérrez, Pathogenesis of dermonecrosis induced by venom of the spitting cobra, Naja nigricollis: An experimental study in mice. Toxicon 119, 171–179 (2016).

13. M. A. Bittenbinder, J. van Thiel, F. C. Cardoso, N. R. Casewell, J.-M. Gutiérrez, J. Kool, F. J. Vonk, Tissue damaging toxins in snake venoms: mechanisms of action, pathophysiology and treatment strategies. *Commun Biol* **7**, 358 (2024).

14. J. M. Gutiérrez, L.-O. Albulescu, R. H. Clare, N. R. Casewell, T. M. Abd El-Aziz, T. Escalante, A. Rucavado, The Search for Natural and Synthetic Inhibitors That Would Complement Antivenoms as Therapeutics for Snakebite Envenoming. *Toxins* **13** (2021), doi:10.3390/toxins13070451.

15. N. R. Casewell, T. N. W. Jackson, A. H. Laustsen, K. Sunagar, Causes and Consequences of Snake Venom Variation. Trends Pharmacol. Sci. 41, 570–581 (2020).

16. T. Hart, A. H. Y. Tong, K. Chan, J. Van Leeuwen, A. Seetharaman, M. Aregger, M. Chandrashekhar, N. Hustedt, S. Seth, A. Noonan, A. Habsid, O. Sizova, L. Nedyalkova, R. Climie, L. Tworzyanski, K. Lawson, M. A. Sartori, S. Alibeh, D. Tieu, S. Masud, P. Mero, A. Weiss, K. R. Brown, M. Usaj, M. Billmann, M. Rahman, M. Constanzo, C. L. Myers, B. J. Andrews, C. Boone, D. Durocher, J. Moffat, Evaluation and Design of Genome-Wide CRISPR/SpCas9 Knockout Screens. G3 7, 2719–2727 (2017).

17. B. Wang, M. Wang, W. Zhang, T. Xiao, C.-H. Chen, A. Wu, F. Wu, N. Traugh, X. Wang, Z. Li, S. Mei, Y. Cui, S. Shi, J. J. Lipp, M. Hinterndorfer, J. Zuber, M. Brown, W. Li, X. S. Liu, Integrative analysis of pooled CRISPR genetic screens using MAGeCKFlute. Nat. Protoc. 14, 756–780 (2019).

18. K. C. J. Nixon, J. Rousseau, M. H. Stone, M. Sarikahya, S. Ehresmann, S. Mizuno, N. Matsumoto, N. Miyake, DDD Study, D. Baralle, S. McKee, K. Izumi, A. L. Ritter, S. Heide, D. Héron, C. Depienne, H. Titheradge, J. M. Kramer, P. M. Campeau, A Syndromic Neurodevelopmental Disorder Caused by Mutations in SMARCD1, a Core SWI/SNF Subunit Needed for Context-Dependent Neuronal Gene Regulation in Flies. Am. J. Hum. Genet. 104, 596–610 (2019).

19. J. Kohoutek, D. Blazek, Cyclin K goes with Cdk12 and Cdk13. Cell Div. 7, 12 (2012).

20. P. J. Watson, L. Fairall, G. M. Santos, J. W. R. Schwabe, Structure of HDAC3 bound to co-repressor and inositol tetraphosphate. Nature 481, 335–340 (2012).

21. T. Fujimoto, K. Doi, M. Koyanagi, T. Tsunoda, Y. Takashima, Y. Yoshida, T. Sasazuki, S. Shirasawa, ZFAT is an antiapoptotic molecule and critical for cell survival in MOLT-4 cells. FEBS Lett. 583, 568–572 (2009).

22. H. W. Jang, S. W. Kim, Y.-J. Cho, K. Heo, B. I. Lee, S. K. Lee, I.-J. Jang, M. G. Lee, W.-J. Kim, J. H. Lee, GWAS identifies two susceptibility loci for lamotrigine-induced skin rash in patients with epilepsy. Epilepsy Res. 115, 88–94 (2015).

23. J. Huang, B. D. Manning, The TSC1-TSC2 complex: a molecular switchboard controlling cell growth. Biochem. J 412, 179–190 (2008).

24. C. C. Dibble, W. Elis, S. Menon, W. Qin, J. Klekota, J. M. Asara, P. M. Finan, D. J. Kwiatkowski, L. O. Murphy, B. D. Manning, TBC1D7 is a third subunit of the TSC1-TSC2 complex upstream of mTORC1. Mol. Cell 47, 535–546 (2012).

25. B. H. Alver, K. H. Kim, P. Lu, X. Wang, H. E. Manchester, W. Wang, J. R. Haswell, P. J. Park, C. W. M. Roberts, The SWI/SNF chromatin remodelling complex is required for maintenance of lineage specific enhancers. Nat. Commun. 8, 14648 (2017).

26. A. Fradet, J. Fitzgerald, INPPL1 gene mutations in opsismodysplasia. J. Hum. Genet. 62, 135–140 (2017).

27. T. Haikonen, M.-L. Rajamäki, J. P. T. Valkonen, Interaction of the microtubule-associated host protein HIP2 with viral helper component proteinase is important in infection with potato virus A. Mol. Plant. Microbe. Interact. 26, 734–744 (2013).

28. T. Touvier, F. Conte-Auriol, O. Briand, C. Cudejko, R. Paumelle, S. Caron, E. Baugé, Y. Rouillé, J.-P. Salles, B. Staels, B. Bailleul, LEPROT and LEPROTL1 cooperatively decrease hepatic growth hormone action in mice. J. Clin. Invest. 119, 3830–3838 (2009).

29. C. Marques, C. A. Reis, R. R. Vivès, A. Magalhães, Heparan Sulfate Biosynthesis and Sulfation Profiles as Modulators of Cancer Signalling and Progression. Front. Oncol. 11, 778752 (2021).

30. S. M. Hoy, L. J. Scott, G. L. Plosker, Tinzaparin sodium: a review of its use in the prevention and treatment of deep vein thrombosis and pulmonary embolism, and in the prevention of clotting in the extracorporeal circuit during haemodialysis. Drugs 70, 1319–1347 (2010).

31. C. J. Dunn, B. Jarvis, Dalteparin: an update of its pharmacological properties and clinical efficacy in the prophylaxis and treatment of thromboembolic disease. Drugs 60, 203–237 (2000).

32. Y. Zhang, Z. Zhao, L. Guan, L. Mao, S. Li, X. Guan, M. Chen, L. Guo, L. Ding, C. Cong, T. Wen, J. Zhao, N-acetyl-heparin attenuates acute lung injury caused by acid aspiration mainly by antagonizing histones in mice. PLoS One 9, e97074 (2014).

33. S. E. Stringer, J. T. Gallagher, Heparan sulphate. Int. J. Biochem. Cell Biol. 29, 709–714 (1997).

34. M. Bernfield, R. Kokenyesi, M. Kato, M. T. Hinkes, J. Spring, R. L. Gallo, E. J. Lose, Biology of the syndecans: a family of transmembrane heparan sulfate proteoglycans. Annu. Rev. Cell Biol. 8, 365–393 (1992).

35. T. D. Kazandjian, D. Petras, S. D. Robinson, J. van Thiel, H. W. Greene, K. Arbuckle, A. Barlow, D. A. Carter, R. M. Wouters, G. Whiteley, S. C. Wagstaff, A. S. Arias, L.-O. Albulescu, A. Plettenberg Laing, C. Hall, A. Heap, S. Penrhyn-Lowe, C. V. McCabe, S. Ainsworth, R. R. da Silva, P. C. Dorrestein, M. K. Richardson, J. M. Gutiérrez, J. J. Calvete, R. A. Harrison, I. Vetter, E. a. B. Undheim, W. Wüster, N. R. Casewell, Convergent evolution of pain-inducing defensive venom components in spitting cobras. Science 371, 386–390 (2021).

36. N. R. Casewell, S. C. Wagstaff, W. Wüster, D. A. N. Cook, F. M. S. Bolton, S. I. King, D. Pla, L. Sanz, J. J. Calvete, R. A. Harrison, Medically important differences in snake venom composition are dictated by distinct postgenomic mechanisms. Proc. Natl. Acad. Sci. U. S. A. 111, 9205–9210 (2014).

37. S. R. Hall, S. A. Rasmussen, E. Crittenden, C. A. Dawson, K. E. Bartlett, A. P. Westhorpe, L.-O. Albulescu, J. Kool, J. M. Gutiérrez, N. R. Casewell, Repurposed drugs and their combinations

prevent morbidity-inducing dermonecrosis caused by diverse cytotoxic snake venoms. Nature Communications 14, 7812 (2023).

38. R. D. Theakston, H. A. Reid, Development of simple standard assay procedures for the characterization of snake venom. Bull. World Health Organ. 61, 949–956 (1983).

39. L.-O. Albulescu, M. S. Hale, S. Ainsworth, J. Alsolaiss, E. Crittenden, J. J. Calvete, C. Evans, M. C. Wilkinson, R. A. Harrison, J. Kool, N. R. Casewell, Preclinical validation of a repurposed metal chelator as an early-intervention therapeutic for hemotoxic snakebite. Sci. Transl. Med. 12 (2020), doi:10.1126/scitranslmed.aay8314.

40. I. S. Khalek, R. R. Senji Laxme, Y. T. K. Nguyen, S. Khochare, R. N. Patel, J. Woehl, J. M. Smith, K. Saye-Francisco, Y. Kim, L. Misson Mindrebo, Q. Tran, M. Kędzior, E. Boré, O. Limbo, M. Verma, R. L. Stanfield, S. K. Menzies, S. Ainsworth, R. A. Harrison, D. R. Burton, D. Sok, I. A. Wilson, N. R. Casewell, K. Sunagar, J. G. Jardine, Synthetic development of a broadly neutralizing antibody against snake venom long-chain α-neurotoxins. Sci. Transl. Med. 16, eadk1867 (2024).

41. C. R. Ferraz, A. Arrahman, C. Xie, N. R. Casewell, R. J. Lewis, J. Kool, F. C. Cardoso, Multifunctional toxins in snake venoms and therapeutic implications: From pain to hemorrhage and necrosis. *Front. Ecol. Evol.* **7** (2019), doi:10.3389/fevo.2019.00218.

42. C. L. Ownby, J. E. Fletcher, T. R. Colberg, Cardiotoxin 1 from cobra (Naja naja atra) venom causes necrosis of skeletal muscle in vivo. Toxicon 31, 697–709 (1993).

43. K. Maduwage, G. K. Isbister, Current treatment for venom-induced consumption coagulopathy resulting from snakebite. PLoS Negl. Trop. Dis. 8, e3220 (2014).

44. V. Paul, A. Pudoor, J. Earali, B. John, C. S. Anil Kumar, T. Anthony, Trial of low molecular weight heparin in the treatment of viper bites. J. Assoc. Physicians India 55, 338–342 (2007).

45. V. Paul, K. A. Prahlad, J. Earali, S. Francis, F. Lewis, Trial of heparin in viper bites. J. Assoc. Physicians India 51, 163–166 (2003).

46. Tin Na Swe, Myint Lwin, Khin Ei Han, Tin Tun, P. e. Tun, Heparin therapy in Russell's viper bite victims with disseminated intravascular coagulation: a controlled trial. Southeast Asian J. Trop. Med. Public Health 23, 282–287 (1992).

47. Myint-Lwin, Tin-Nu-Swe, Myint-Aye-Mu, Than-Than, Thein-Than, Tun-Pe, Heparin therapy in Russell's viper bite victims with impending dic (a controlled trial). Southeast Asian J. Trop. Med. Public Health 20, 271–277 (1989).

48. H. V. Patel, A. A. Vyas, K. A. Vyas, Y. S. Liu, C. M. Chiang, L. M. Chi, W. g. Wu, Heparin and heparan sulfate bind to snake cardiotoxin. Sulfated oligosaccharides as a potential target for cardiotoxin action. J. Biol. Chem. 272, 1484–1492 (1997).

49. A. A. Vyas, J. J. Pan, H. V. Patel, K. A. Vyas, C. M. Chiang, Y. C. Sheu, J. K. Hwang, W. g. Wu, Analysis of binding of cobra cardiotoxins to heparin reveals a new beta-sheet heparin-binding structural motif. J. Biol. Chem. 272, 9661–9670 (1997).

50. R. D. Higginbotham, Mast cells and local resistance to Russell's viper venom. J. Immunol. 95, 867–875 (1965).

51. P. A. Melo, G. Suarez-Kurtz, Release of sarcoplasmic enzymes from skeletal muscle by Bothrops jararacussu venom: antagonism by heparin and by the serum of South American marsupials. Toxicon 26, 87–95 (1988).

52. P. A. Melo, M. I. Homsi-Brandeburgo, J. R. Giglio, G. Suarez-Kurtz, Antagonism of the myotoxic effects of Bothrops jararacussu venom and bothropstoxin by polyanions. Toxicon 31, 285–291 (1993).

53. B. Lomonte, E. Moreno, A. Tarkowski, L. A. Hanson, M. Maccarana, Neutralizing interaction between heparins and myotoxin II, a lysine 49 phospholipase A2 from Bothrops asper snake venom. Identification of a heparin-binding and cytolytic toxin region by the use of synthetic peptides and molecular modeling. J. Biol. Chem. 269, 29867–29873 (1994).

54. B. Lomonte, G. León, Y. Angulo, A. Rucavado, V. Núñez, Neutralization of Bothrops asper venom by antibodies, natural products and synthetic drugs: contributions to understanding snakebite envenomings and their treatment. Toxicon 54, 1012–1028 (2009).

55. T. M. Clausen, D. R. Sandoval, C. B. Spliid, J. Pihl, H. R. Perrett, C. D. Painter, A. Narayanan, S. A. Majowicz, E. M. Kwong, R. N. McVicar, B. E. Thacker, C. A. Glass, Z. Yang, J. L. Torres, G. J. Golden, P. L. Bartels, R. N. Porell, A. F. Garretson, L. Laubach, J. Feldman, X. Yin, Y. Pu, B. M. Hauser, T. M. Caradonna, B. P. Kellman, C. Martino, P. L. S. M. Gordts, S. K. Chanda, A. G. Schmidt, K. Godula, S. L. Leibel, J. Jose, K. D. Corbett, A. B. Ward, A. F. Carlin, J. D. Esko, SARS-CoV-2 Infection Depends on Cellular Heparan Sulfate and ACE2. Cell 183, 1043–1057.e15 (2020).

56. D. Shukla, J. Liu, P. Blaiklock, N. W. Shworak, X. Bai, J. D. Esko, G. H. Cohen, R. J. Eisenberg, R. D. Rosenberg, P. G. Spear, A novel role for 3-O-sulfated heparan sulfate in herpes simplex virus 1 entry. Cell 99, 13–22 (1999).

57. A. Volland, M. Lohmüller, E. Heilmann, J. Kimpel, S. Herzog, D. von Laer, Heparan sulfate proteoglycans serve as alternative receptors for low affinity LCMV variants. PLoS Pathog. 17, e1009996 (2021).

58. C. J. Blondel, J. S. Park, T. P. Hubbard, A. R. Pacheco, C. J. Kuehl, M. J. Walsh, B. M. Davis, B. E. Gewurz, J. G. Doench, M. K. Waldor, CRISPR/Cas9 Screens Reveal Requirements for Host Cell Sulfation and Fucosylation in Bacterial Type III Secretion System-Mediated Cytotoxicity. Cell Host Microbe 20, 226–237 (2016).

59. G. Roderiquez, T. Oravecz, M. Yanagishita, D. C. Bou-Habib, H. Mostowski, M. A. Norcross, Mediation of human immunodeficiency virus type 1 binding by interaction of cell surface heparan sulfate proteoglycans with the V3 region of envelope gp120-gp41. J. Virol. 69, 2233–2239 (1995).

60. S. Sarrazin, W. C. Lamanna, J. D. Esko, Heparan sulfate proteoglycans. Cold Spring Harb. Perspect. Biol. 3 (2011), doi:10.1101/cshperspect.a004952.

61. K. E. Bartlett, S. R. Hall, S. A. Rasmussen, E. Crittenden, C. A. Dawson, L.-O. Albulescu, W. Laprade, R. A. Harrison, A. J. Saviola, C. M. Modahl, T. P. Jenkins, M. C. Wilkinson, J. M. Gutiérrez, N. R. Casewell, Dermonecrosis caused by a spitting cobra snakebite results from toxin potentiation and is prevented by the repurposed drug varespladib. *Proc. Natl. Acad. Sci. U. S. A.* **121**, e2315597121 (2024).

62. S. K. Menzies, T. Litschka-Koen, R. J. Edge, J. Alsolaiss, E. Crittenden, S. R. Hall, A. Westhorpe, B. Thomas, J. Murray, N. Shongwe, S. Padidar, D. G. Lalloo, N. R. Casewell, J. Pons, R. A. Harrison, Two snakebite antivenoms have potential to reduce Eswatini's dependency upon a single, increasingly unavailable product: Results of preclinical efficacy testing. PLoS Negl. Trop. Dis. 16, e0010496 (2022).

63. A. B. Nair, S. Jacob, A simple practice guide for dose conversion between animals and human. J. Basic Clin. Physiol. Pharmacol. 7, 27–31 (2016).

64. A. Grainger, Low molecular weight heparinsLancashire and South Cumbria Medicines Management Group (available at https://www.lancsmmg.nhs.uk/medicines-library/low-molecular-weight-heparins/).

65. F. E. Grubbs, Procedures for Detecting Outlying Observations in Samples. Technometrics 11, 1–21 (1969).

66. I. Colombo, E. Sangiovanni, R. Maggio, C. Mattozzi, S. Zava, Y. Corbett, M. Fumagalli, C. Carlino, P. A. Corsetto, D. Scaccabarozzi, S. Calvieri, A. Gismondi, D. Taramelli, M. Dell'Agli, HaCaT Cells as a Reliable In Vitro Differentiation Model to Dissect the Inflammatory/Repair Response of Human Keratinocytes. Mediators Inflamm. 2017, 7435621 (2017).

67. V. G. Wilson, Growth and differentiation of HaCaT keratinocytes. Methods Mol. Biol. 1195, 33–41 (2014).

68. L. Loo, M. A. Waller, C. L. Moreno, A. J. Cole, A. O. Stella, O.-T. Pop, A.-K. Jochum, O. H. Ali, C. E. Denes, Z. Hamoudi, F. Chung, A. Aggarwal, J. K. K. Low, K. Patel, R. Siddiquee, T. Kang, S. Mathivanan, J. P. Mackay, W. Jochum, L. Flatz, D. Hesselson, S. Turville, G. G. Neely, Fibroblast-expressed LRRC15 is a receptor for SARS-CoV-2 spike and controls antiviral and antifibrotic transcriptional programs. PLoS Biol. 21, e3001967 (2023).

69. J. Joung, S. Konermann, J. S. Gootenberg, O. O. Abudayyeh, R. J. Platt, M. D. Brigham, N. E. Sanjana, F. Zhang, Genome-scale CRISPR-Cas9 knockout and transcriptional activation screening. Nat. Protoc. 12, 828–863 (2017).

70. D. Conant, T. Hsiau, N. Rossi, J. Oki, T. Maures, K. Waite, J. Yang, S. Joshi, R. Kelso, K. Holden, B. L. Enzmann, R. Stoner, Inference of CRISPR Edits from Sanger Trace Data. CRISPR J 5, 123–130 (2022).

Acknowledgments: We would like to give our thanks to Paul Rowley for maintaining the snakes at the LSTM's herpetarium and for routine venom extractions, Cassandra Modahl for her help with animal welfare observations, Michael Abouyannis for discussions relating to clinical use of heparins, and Valerie Tilston and her team at the University of Liverpool for preparing the histopathology slides. The authors also acknowledge use of the Biomedical Services Unit provided by Liverpool Shared Research Facilities. We also thank Sydney Analytical, Sydney Mass Spectrometry and Sydney Cytometry for their support, and Geoffrey Maranga from the Kenyan Snakebite Research and Interventions Centre for the snake images. Figure illustrations were created with BioRender.com.

Funding:

The laboratory of GGN is supported by the National Health and Medical Research Council Ideas Grant (2020532 to GGN) and Australian Research Council Discovery Project Grant (DP220103530 to GGN). SRH was supported by the Newton International Fellowship from the Royal Society (NIF\R1\192161 to SRH). The laboratory of NRC was supported by a Wellcome Trust project grant (221712/Z/20/Z to NRC) and a UK Medical Research Council research grant (MR/S00016X/1 to NRC). NRC is also supported by a Sir Henry Dale Fellowship jointly funded by the Wellcome Trust and the Royal Society (200517/Z/16/Z to NRC).

Author contributions:

Conceptualization: GGN, NRC

Methodology: TYD, SRH, FC, SK, KP, L-OA, MCW, JMG, NRC, GGN

Investigation: TYD, SRH, FC, SK, EC, KP, CAD, APW, KEB, SAR, AEM, MCW, NRC, JMG

Visualization: TYD, SRH, CED, NRC, GGN

Funding acquisition: SRH, GGN, NRC

Supervision: CLM, CED, JPM, MCW, NRC, JMG, GGN

Writing – original draft: TYD, GGN, SRH, NRC

Writing – review & editing: TYD, SRH, FC, SK, EC, KP, CAD, APW, KEB, SAR, CLM, CED, L-OA, AEM, JPM, MCW, JMG, NRC, GGN

Competing interests: A provisional patent application ("A new broad acting antidote for venom-induced injury including local tissue damage and/or skin irritation", application number: 2024900779) has been submitted by GGN, NRC, FC and TYD based on these results. The other authors declare that they have no competing interests.

Data and materials availability: All data are available in the main text or the supplementary materials. Whole genome CRISPR KO sequencing datasets have been deposited in GEO with the identifier GSE262798.

Figure legends

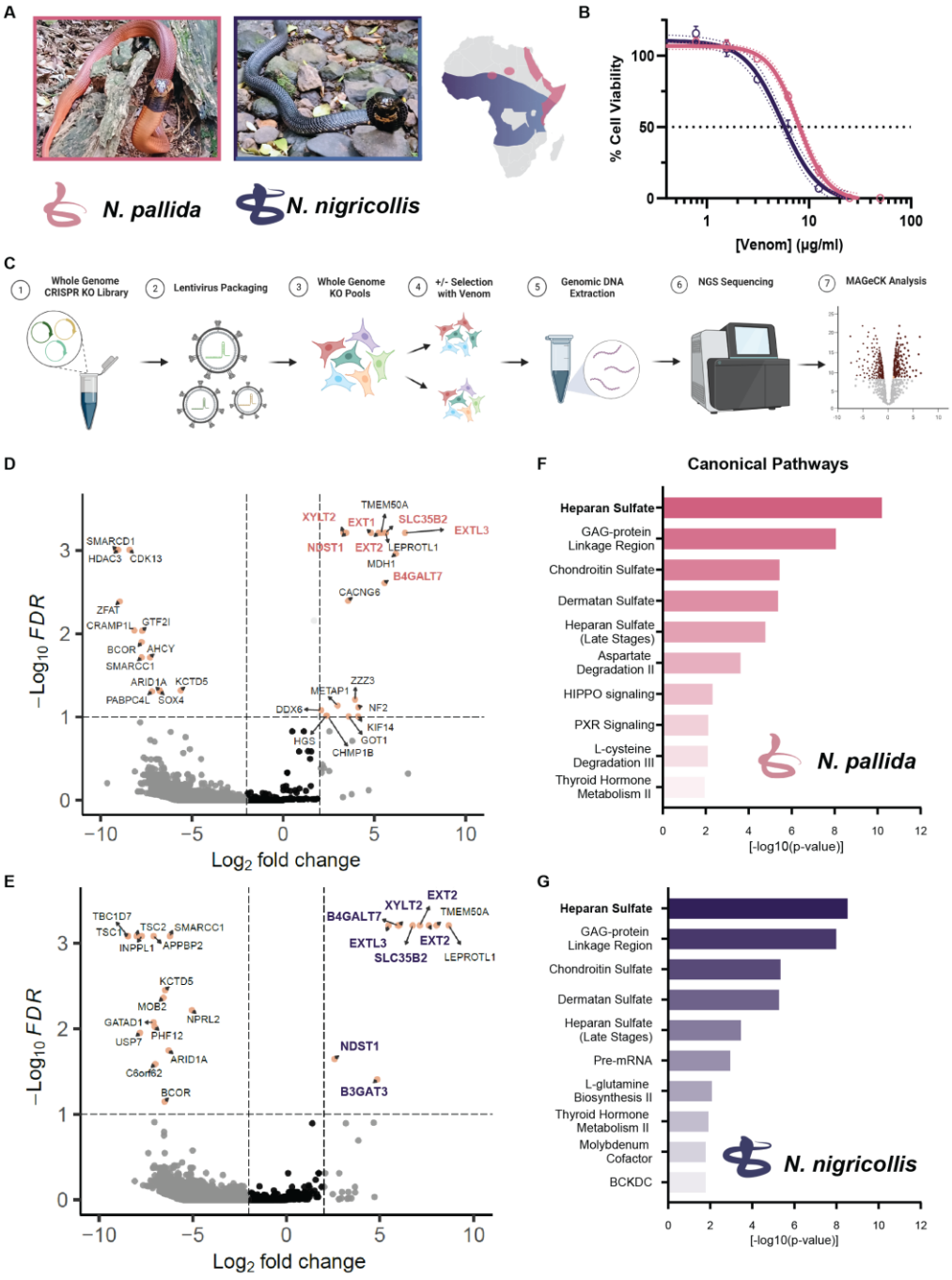

Fig. 1. An in vitro whole genome CRISPR-Cas9 knockout screen identifies genes required for African spitting cobra venom cytotoxicity. (**A**) Red spitting cobra (*Naja pallida*) and black-necked spitting cobra (*Naja nigricollis*) and their distributions. (**B**) HAP1 cell viability as determined by resazurin assays after 24 h treatment with serial dilutions of spitting cobra venoms (n = 3). (**C**) Schematic of pooled CRISPR knockout library screens. HAP1 cells were transduced with a whole genome knockout library at MOI = 0.3. Venom was added to library cells and

genomic DNA extracted from selected and unselected control populations before undergoing next generation sequencing. Analysis was calculated using the MAGeCK pipeline. (**D and E**) Gene enrichment analysis of screens using (D) venom from *N. pallida*, and (E) venom from *N. nigricollis*, performed using MAGeCK (*17*) Horizontal dotted lines indicate $-\log_{10}$(false discovery rate) (FDR) = 1 and vertical dotted lines indicate $\log_2$(fold changes) (LFCs) of -2 and 2. Plots were generated using EnhancedVolcano (v1.10.0) R package. (**F and G**) Top canonical pathways identified through Ingenuity Pathway Analysis (IPA). (F) using venom from *N. pallida*, and (G) using venom from *N. nigricollis*. Photographs in panel A are by Geoffrey Maranga, schematic in panel C created with BioRender.com.

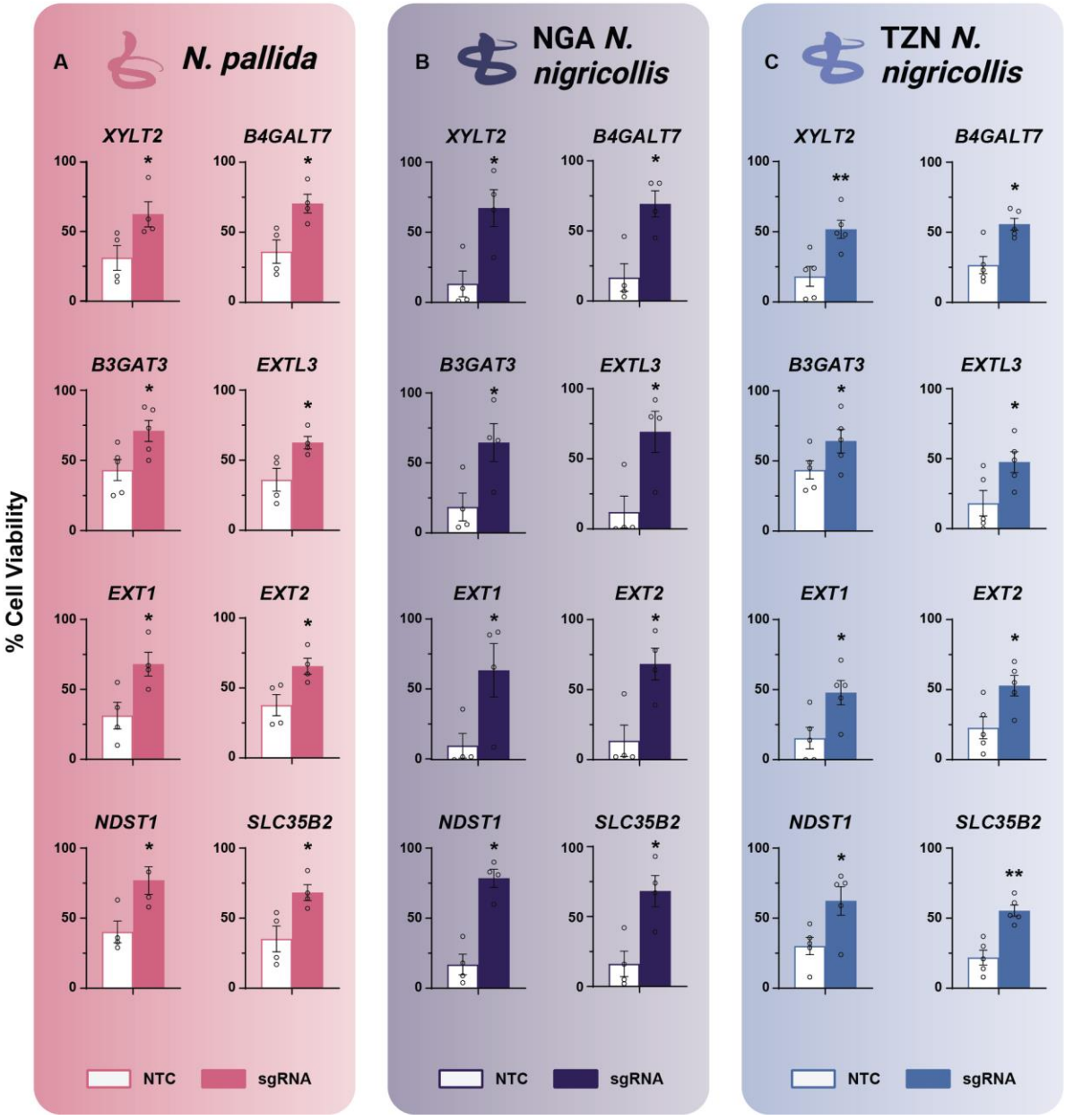

Fig. 2. Heparan sulfate biosynthesis is required for spitting cobra venom cytotoxicity. (**A to C**) Pools of single sgRNA knockout cells for heparan sulfate biosynthesis hits (*XYLT2*, *B4GALT7*, *B3GAT3*, *EXTL3*, *EXT1*, *EXT2*, *NDST1* and *SLC35B2*) and a non-targeting control sgRNA (NTC) were generated via lentiviral transduction in HAP1 cells. Pooled knockout cells were treated with 10 μg/mL *N. pallida* (**A**), Nigerian (NGA) *N. nigricollis* (**B**), or Tanzanian

(TZN) *N. nigricollis* (**C**) venom for 24 h and viability ascertained using resazurin. Significance was determined by one-tailed Mann-Whitney test, *P<0.05, **P<0.01 (n = 4-5).

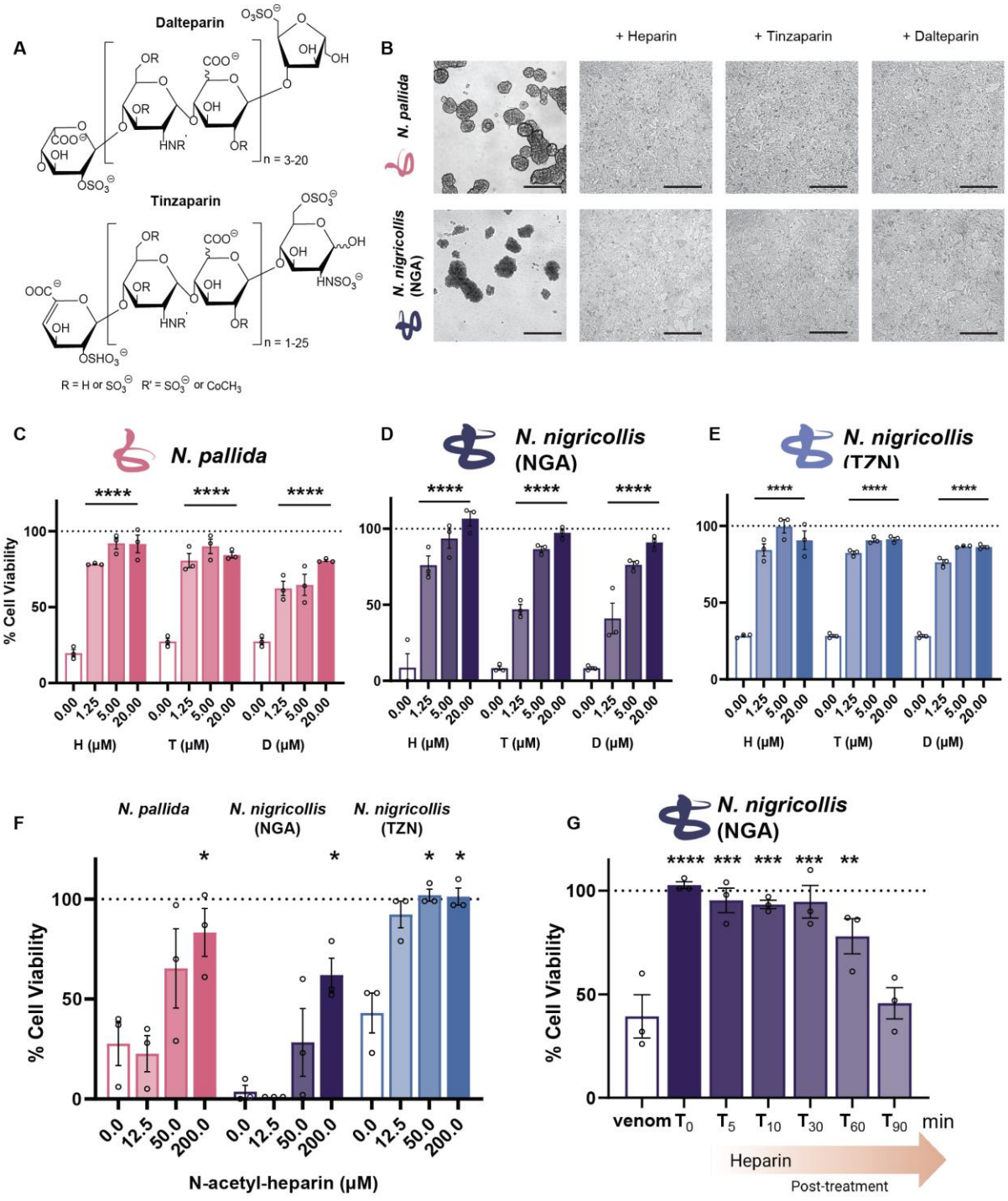

Fig. 3. Heparin and LMW heparinoids block *Naja* venom action in vitro. (**A**) Chemical structures of the low molecular weight heparinoids, dalteparin and tinzaparin. (**B**) Representative brightfield microscopy of HAP1 cells after 24 h exposure to 10 μg/mL *N. pallida* (top) or Nigerian (NGA) *N. nigricollis* venom (bottom), simultaneously treated with 20 μM heparin, tinzaparin or dalteparin. Scale bar = 200 μm (**C to E**) Venoms (10 μg/mL) and serial dilutions of

heparin (H), tinzaparin (T) or dalteparin (D) (1.25-20 μM) were added simultaneously to HAP1 cells. Resazurin cell viability assays were performed after 24 h of treatment. Significance was determined by two-way analysis of variance (ANOVA) and Dunnett test, ****P<0.0001 (*n* = 3). (**F**) Venoms (10 μg/mL) and serial dilutions of N-acetyl-heparin (12.5-200 μM) added simultaneously to HAP1 cells. Resazurin cell viability assays were performed after 24 h of treatment. Significance was determined by two-way ANOVA and Dunnett test, *P<0.05 (*n* = 3). (**G**) HAP1 cells were treated with 10 μg/mL *N. nigricollis* (NGA) venom before addition of 20 μM heparin immediately after, or 5-, 10-, 30-, 60- or 90-min post venom application. Significance was determined by ordinary one-way ANOVA and Dunnett test, **P<0.01, ***P<0.001, ****P<0.0001 (*n* = 3).

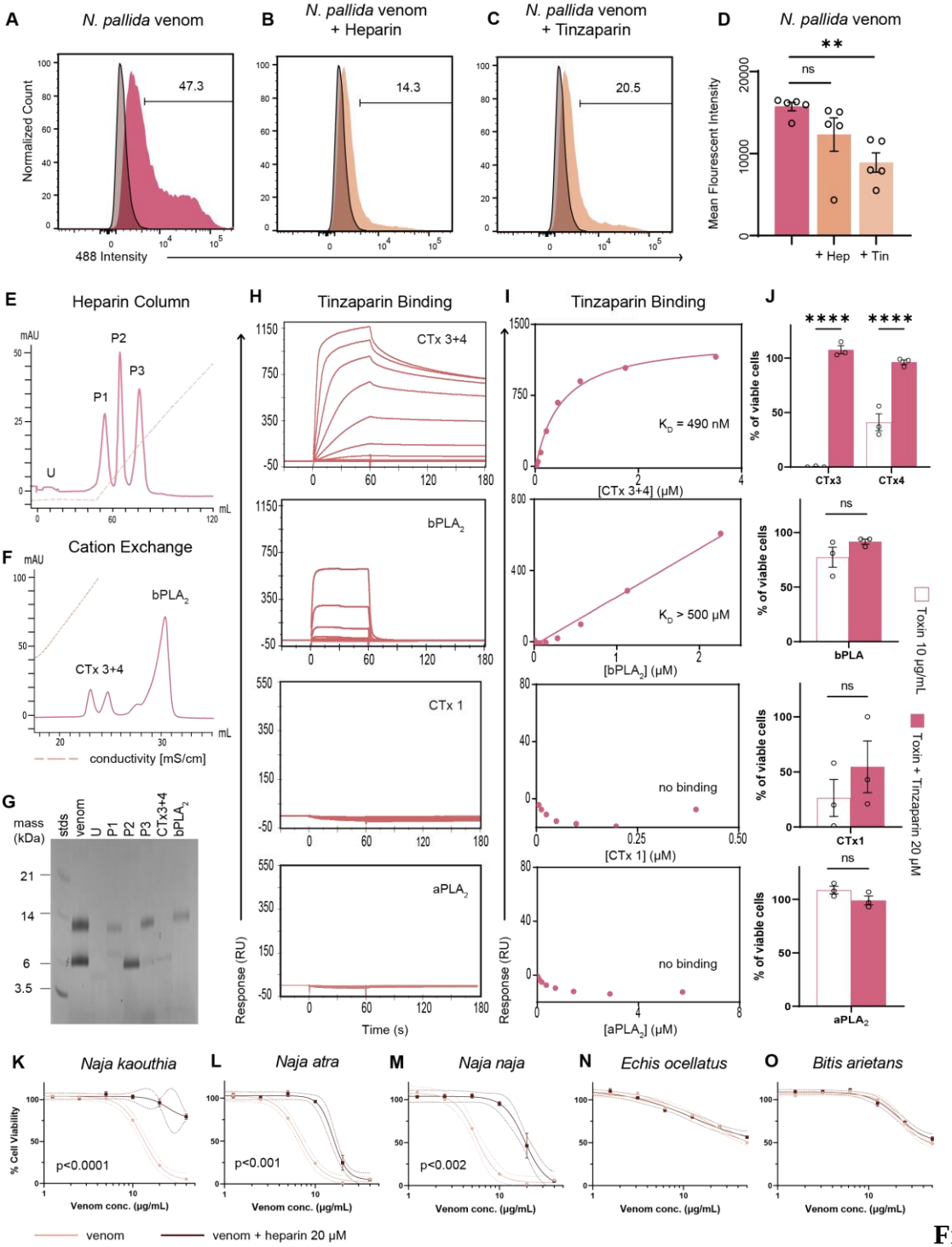

Fig. 4.

Heparin binds 3FTxs and prevents their cytotoxicity. (**A**) Representative flow cytometry histograms of WT HAP1 cells in gray and cells exposed to Alexa488-tagged *N. pallida* venom, (**B**) with venom and heparin (**C**) with venom and tinzaparin. (**D**) Quantification of binding intensity (n = 5). Significance was determined by one-way ANOVA and Dunnett test, **P<0.01.

(**E**) Heparin affinity chromatography of *N. pallida* venom. Unbound (U), Peak 1 (P1), Peak 2 (P2) and Peak 3 (P3). (**F**) Cation exchange chromatography of Peak 3. (**G**) SDS-PAGE gel of whole venom and resulting toxin fractions. (**H**) Surface plasmon resonance (SPR). Representative normalized sensorgrams of toxin binding to heparin. The specific toxin is indicated in the upper right corner of each sensorgram (**I**) Fits of the SPR data from (**H**) to a 1:1 binding model are shown and K_Ds are indicated on each plot. (**J**) Cytotoxicity of 10 μg/mL of each toxin fractions either without (left) or with (right) addition of 20 μM heparin. Significance determined by two-way ANOVA and Sidak test, ****P<0.0001 (*n* = 3). (**K to M**) Cytotoxicity of venoms containing 3FTxs (**K,** *Naja kaouthia;* **L,** *Naja atra;* **M,** *Naja naja*) without (tan) or with (brown) addition of heparin. (**N and O**) Cytotoxicity of venoms from more distantly related snakes without (tan) or with (brown) addition of heparin (**N**, *Echis ocellatus;* **O,** *Bitis arietans*). Significance was determined by simple linear regression.

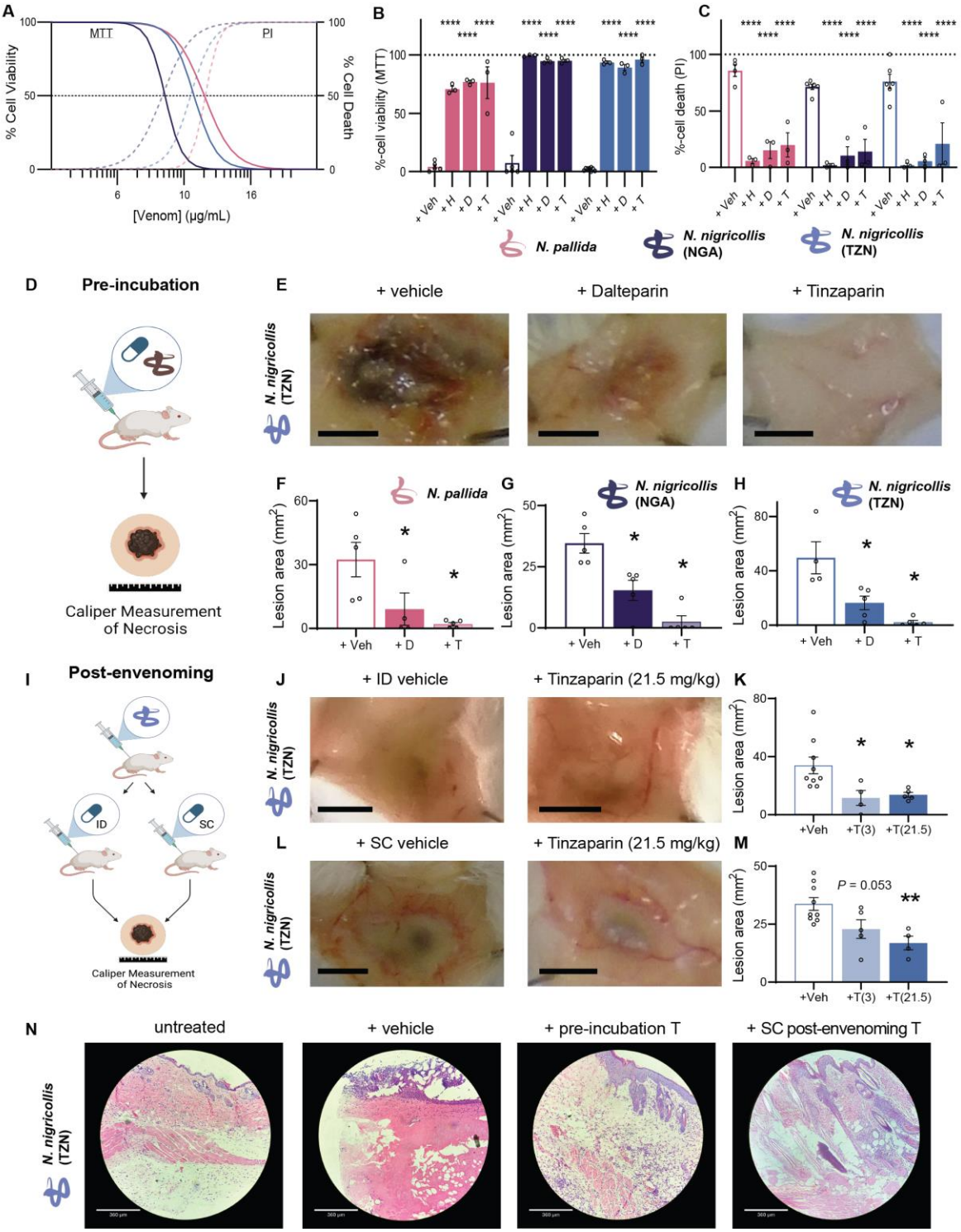

Fig. 5. Snake venom-induced dermonecrosis is inhibited by heparinoids in vivo. (**A**) 3-(4,5-dimethylthiazol-2-yl)-2,5 diphenyl tetrazolium bromide (MTT) cell viability and propidium iodide (PI) cell death assays on HaCaT epidermal keratinocytes exposed to serial dilutions (4.74-47.4 µg/mL) of spitting cobra venoms. (**B**) MTT-quantified percentage cell viability and (**C**) PI-quantified percentage cell death of HaCaT keratinocytes treated with venoms (*N. pallida* 15

μg/mL, NGA *N. nigricollis* 10 μg/mL, and TZN *N. nigricollis* 15 μg/mL) preincubated with saline vehicle control or heparin, dalteparin or tinzaparin (1000 μg/mL). (**D**) Schematic of the pre-incubation experiment. Mice were ID-injected with venom that had been pre-incubated with saline vehicle control, dalteparin (60 μg [3 mg/mL]) or tinzaparin (60 μg [3 mg/mL]). After 72 h mice were euthanized and the skin lesions excised for photographs and height and width measurements with calipers, from which area was calculated (bar graphs represent the mean lesion area for each treatment group and error bars represent SEM). (**E**) Representative images of necrosis, scale bar = 5 mm. Calculated lesion areas for (**F**) 25 μg *N. pallida*, (**G**) 57 μg Nigerian *N. nigricollis*, or (**H**) 63 μg Tanzanian *N. nigricollis* venom, n = 4-5 (significance was determined by one-way ANOVA and Dunnett test, *P<0.05, **P<0.01). (**I**) Schematic of the post-envenoming treatment experiment. Mice were ID-injected with Tanzanian *N. nigricollis* venom (63 μg) immediately followed by either ID-injected saline vehicle control or tinzaparin at low dose (3 mg/kg) or moderate 'human-equivalent' dose (21.5 mg/kg) at the venom injection site, or by SC-injected saline vehicle control or tinzaparin at low dose (3 mg/kg) or moderate 'human-equivalent' dose (21.5 mg/kg) underneath the venom injection site. (**J**) Representative images of dermonecrosis in mice ID-injected with Tanzanian *N. nigricollis* venom (63 μg) immediately followed by ID-injection of saline vehicle control (left) or moderate 'human-equivalent' dose (21.5 mg/kg) tinzaparin (right) Scale bar = 5 mm. **(K)** Calculated lesion areas. (**L**) Representative images of dermonecrosis in mice ID-injected with Tanzanian *N. nigricollis* venom (63 μg) immediately followed by SC-injection of saline vehicle control (left) or moderate 'human-equivalent' dose (21.5 mg/kg) tinzaparin (right). Scale bar = 5 mm. (M) Calculated lesion areas. (**N**) Light micrograph images (100X, scale bar = 360 μm) of hematoxylin & eosin (H&E)-stained skin lesion cross-sections from untreated mice (left), mice injected with Tanzanian *N. nigricollis* venom (63 μg) and pre-incubated saline vehicle control (second from left, mice injected with venom pre-incubated with tinzaparin (3 mg/kg) (second from right), and mice SC-injected with tinzaparin (21.5 mg/kg) immediately post-envenoming (right). Schematic in panel D and I created with BioRender.com